10.1098/rspa.2001.0785

THE ROYAL SOCIETY

Vortex instability from a near-vertical heated surface in a porous medium. I Linear instability

By D. Andrew S. Rees

Department of Mechanical Engineering, University of Bath, Claverton Down, Bath BA2 7AY, UK

Received 22 May 2000; accepted 18 January 2001

In this paper we consider the stability of thermal boundary-layer flow in a porous medium. In particular, we are concerned about the susceptibility of streamwise vortex disturbances to growth when the heated surface is very close to the vertical. This regime allows both the basic flow and the disturbance equations to satisfy the boundary-layer approximation, and hence the present analysis forms a mathematically consistent framework. It is shown that the usual method of analysing linear instability is too restrictive and that disturbances grow from positions much closer to the leading edge than are predicted using the parallel flow approximation.

Keywords: vortex instabilities; linear theory; porous media; boundary layer

1. Introduction

In this paper we address one aspect of the classical problem of determining criteria for the onset of instability in the free convective thermal boundary-layer flow from an inclined heated surface embedded in an otherwise cold porous medium. This problem was considered first by Hsu & Cheng (1979) and re-examined by Jang & Chang (1988), but many other papers considering variations on the general theme are quoted in the review article by Rees (1998).

The traditional method for analysing such stability problems proceeds initially by forming a set of perturbation equations for small-amplitude disturbances to the basic flow. The next step involves a specification of how the disturbance varies in the streamwise direction and a Fourier decomposition of the disturbance (which is in the spanwise direction for streamwise vortices or in the streamwise direction for travelling waves). This results in an ordinary differential eigenvalue problem for the disturbance, where the eigenvalue, a function of wavenumber, is the streamwise position corresponding to neutrality. Such a procedure, although very widely applied, assumes too much about the form of the disturbance. Although a Fourier decomposition is very reasonable for the analysis of streamwise vortices, it is suspect in the case of waves, as the basic flow does not have parallel streamlines. Similarly, the non-parallel nature of the basic flow means that there is no *a priori* rationale for specifying the streamwise variation of the disturbance. Furthermore, there is also a major mathematical inconsistency between the application of the boundary-layer approximation (which implies that x, the streamwise coordinate, is asymptotically

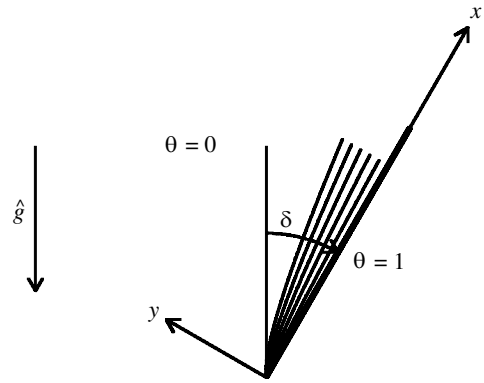

Figure 1. Sketch of the flow domain and boundary conditions.

large) and the result of the stability analysis (which yields a finite value for x). But the popularity of the method lies in the fact that it often gives reasonable results.

It was shown in Storesletten & Rees (1998) that stability analyses along the above lines become increasingly reliable as the inclination of the heated surface tends towards the vertical. In that paper the authors considered the effects of using a third-order boundary-layer theory to describe the basic flow as a means of assessing by how much the accuracy of the description of the basic flow affects the stability criterion. Here we study the case of a near-vertical surface, since the leading-order boundary-layer flow is particularly accurate in this limit. It is also the case that the point of neutral stability recedes to infinity in the same limit. Indeed, we show that the near-vertical limit allows both the basic flow and perturbation analysis to proceed in a mathematically consistent manner.

We find that the streamwise evolution of disturbances is given by the solution of a parabolic system of partial differential equations. Therefore, it is possible to compare directly a consistent approach to the linear stability problem with the older-fashioned method involving ordinary differential eigenvalue problems. In this regard, the present work is similar to that of Hall (1983). We show that the traditional method yields qualitatively correct results, but it yields critical distances that are somewhat larger than those obtained using the parabolic system.

2. Equations of motion and basic flow

We consider the stability of the boundary-layer flow induced by a uniform temperature heated surface embedded in a fluid-saturated porous medium. The fluid motion is assumed to be governed by Darcy's law, while boundary and inertia effects, as modelled by the Brinkman and Forchheimer terms, are taken to be negligible. The fluid is Boussinesq, and the fluid and porous matrix are assumed to be in local thermal equilibrium. The non-dimensional equations of motion were presented by Riley & Rees (1985) in the form

$$\bar{u}_{\bar{x}} + \bar{v}_{\bar{y}} + \bar{w}_{\bar{z}} = 0, \tag{2.1 a}$$

$$\bar{u} = -\bar{P}_{\bar{x}} + \bar{\theta}\cos\delta, \tag{2.1 b}$$

$$\bar{v} = -\bar{P}_{\bar{y}} + \bar{\theta}\sin\delta, \tag{2.1 c}$$

$$\bar{w} = -\bar{P}_{\bar{z}}, \tag{2.1 d}$$

$$\bar{\theta}_{\bar{t}} + \bar{u}\bar{\theta}_{\bar{x}} + \bar{v}\bar{\theta}_{\bar{y}} + \bar{w}\bar{\theta}_{\bar{z}} = \nabla^2\bar{\theta}. \tag{2.1 e}$$

Here, $\bar{x}$, $\bar{y}$ and $\bar{z}$ are the streamwise, cross-stream and spanwise Cartesian coordinates, and $\bar{u}$, $\bar{v}$ and $\bar{w}$ are the corresponding fluid flux velocities. The pressure is $\bar{P}$ and temperature is $\bar{\theta}$. In (2.1 *b*) and (2.1 *c*), the angle of inclination of the semi-infinite surface from the vertical is δ, where $0 < \delta < \frac{1}{2}\pi$ corresponds to an upward-facing surface with the leading edge placed vertically below the rest of the surface. The configuration is illustrated in figure 1. Equations (2.1) have been non-dimensionalized in such a way that the porous medium Rayleigh number has been set equal to 1. Such a device, which is discussed in some detail in the review by Rees (1998), is equivalent to having a natural length-scale based upon the fluid and matrix properties; thus a non-dimensional length of precisely 1 is equivalent to the dimensional length, L, given by

$$L^{-1} = \rho\hat{g}\beta K\Delta T/\mu\alpha, \tag{2.2}$$

where ρ is a reference density, $\hat{g}$ is acceleration due to gravity, β is the volumetric coefficient of expansion, K is permeability, ΔT is the temperature drop between the heated surface and the ambient fluid, μ is the fluid viscosity and α is the thermal diffusivity of the saturated medium.

The main interest of this paper is to develop a formal asymptotic theory of vortex instability in the limit of small inclinations from the vertical. Storesletten & Rees (1998), in a stability analysis which involves higher-order approximations to the basic flow, show that the critical distance from the leading edge beyond which vortex disturbances grow is given by

$$\bar{x}_{\mathrm{c}} \simeq 110.7\left(\frac{\cos\delta}{\sin^2\delta}\right), \tag{2.3}$$

when using only the leading-order basic flow. Hsu & Cheng (1979) analysed the same stability problem much earlier and obtained the same result, but with the numerical coefficient equal to 120.7, using slightly different assumptions. The associated wavenumbers which minimize the critical distance were also slightly different from one another. Therefore, as the inclination angle, δ, becomes small, the point of incipient instability recedes from the origin. In this limit, the accuracy of the boundary-layer approximation improves and therefore it is necessary to consider only the leading-order flow in the present paper. The wavenumber of the vortex disturbances in both papers was shown to be proportional to $\sin\delta$.

Given the above observations, we may introduce the following rescalings,

$$\left.\begin{gathered} \bar{x} = \left(\frac{\cos\delta}{\sin^2\delta}\right)x, \qquad \bar{y} = \left(\frac{1}{\sin\delta}\right)y, \qquad \bar{z} = \left(\frac{1}{\sin\delta}\right)z, \\ \bar{u} = (\cos\delta)u, \qquad \bar{v} = (\sin\delta)v, \qquad \bar{w} = (\sin\delta), \\ \bar{P} = P, \qquad \bar{\theta} = \Theta, \qquad \bar{t} = \left(\frac{1}{\sin^2\delta}\right)t, \end{gathered}\right\} \tag{2.4}$$

into (2.1) to obtain

$$u_x + v_y + w_z = 0, \tag{2.5 a}$$

$$u = \Theta - \left(\frac{\sin^2\delta}{\cos^2\delta}\right)P_x, \tag{2.5 b}$$

$$v = \Theta - P_y, \tag{2.5 c}$$

$$w = -P_z, \tag{2.5 d}$$

$$\Theta_t + u\Theta_x + v\Theta_y + w\Theta_z = \left(\frac{\sin^2\delta}{\cos^2\delta}\right)\Theta_{xx} + \Theta_{yy} + \Theta_{zz}. \tag{2.5 e}$$

The limiting case, $\delta \to 0$, may now be seen as being equivalent to invoking the boundary-layer approximation, since, in this limit, the length-scale represented by $x = 1$ is asymptotically greater than that represented by $y = 1$ (see equations (2.4)).

The basic flow whose stability we analyse may be formulated in two different ways, either in a streamfunction/temperature formulation (which takes advantage of the fact that the basic flow is steady and two dimensional) or in a pressure/temperature formulation (which is necessary for the three-dimensional stability analysis). If we assume that all z and t derivatives are zero and set

$$u = \psi_y \quad \text{and} \quad v = -\psi_x \tag{2.6}$$

into (2.5), with $\delta \to 0$, then we obtain the following equations:

$$\psi_y = \Theta, \tag{2.7 a}$$

$$\Theta_{yy} = \psi_y\Theta_x - \psi_x\Theta_y, \tag{2.7 b}$$

$$p_y = \Theta + \psi_x. \tag{2.7 c}$$

The similarity solution takes the form

$$\psi = x^{1/2}f(\eta), \qquad \Theta = g(\eta), \qquad P = q_1(\eta) + x^{1/2}q_2(\eta), \tag{2.8}$$

where

$$\eta = y/x^{1/2}. \tag{2.9}$$

The variable η is the vertical similarity variable, which was given originally by Cheng & Minkowycz (1977) using an analysis involving the local Rayleigh number. The equations satisfied by f, g and q are

$$f' = g, \tag{2.10 a}$$

$$g'' + \tfrac{1}{2}fg' = 0, \tag{2.10 b}$$

$$q_1' = \tfrac{1}{2}(f - \eta f'), \tag{2.10 c}$$

$$q_2' = g, \tag{2.10 d}$$

subject to the boundary conditions

$$f(0) = 0, \quad g(0) = 1 \quad \text{and} \quad g(\eta) \to 0 \quad \text{as } \eta \to \infty. \tag{2.11}$$

Boundary conditions for q_1 and q_2 need not be specified, as the definitions of q_1' and q_2' are all that is required in the linear stability analysis later. The solution of (2.10 *a*), (2.10 *b*) was given in Cheng & Minkowycz (1977) and have appeared in many subsequent papers, but we note that $g'(0) = -0.443\,75$ to five significant figures.

Having obtained the basic flow using the streamfunction/temperature form, the vortex stability analysis requires that the full governing equations (in the limit as $\delta \to 0$) be written in the pressure/temperature form,

$$P'' + \xi^2 P_{zz} = \tfrac{1}{2}(\xi\Theta_\xi - \eta\Theta') + \xi\Theta', \tag{2.12 a}$$

$$\Theta'' + \xi^2\Theta_{zz} = \tfrac{1}{2}(\xi\Theta_\xi - \eta\Theta')\Theta - P'\Theta' + \xi\Theta\Theta' + \xi^2(\Theta_t - P_z\Theta_z), \tag{2.12 b}$$

subject to the boundary conditions

$$\eta = 0: \quad P' = 1, \quad \Theta = 1,$$
$$\eta \to \infty: \quad P, \Theta \to 0.$$

The $\eta = 0$ pressure condition may be deduced from (2.5 *c*). In (2.12), primes denote derivatives with respect to η, and ξ has been defined according to

$$\xi = x^{1/2}, \tag{2.13}$$

for notational and numerical convenience.

3. Perturbation analysis

Beginning with (2.12), we perturb about the basic solution given by (2.8) by setting

$$P = q_1(\eta) + \xi q_2(\eta) + \hat{p}(\xi, \eta, z), \tag{3.1 a}$$

$$\Theta = f'(\eta) + \hat{\theta}(\xi, \eta, z, t) \tag{3.1 b}$$

to obtain the following full disturbance equations,

$$\hat{p}'' + \xi^2\hat{p}_{zz} = \tfrac{1}{2}(\xi\hat{\theta}_\xi - \eta\hat{\theta}') + \xi\hat{\theta}', \tag{3.2 a}$$

$$\begin{aligned}\hat{\theta}'' + \xi^2\hat{\theta}_{zz} = {} & (\tfrac{1}{2}f')\xi\hat{\theta}_\xi - (\tfrac{1}{2}f)\hat{\theta}' + (f'')(\xi - \tfrac{1}{2}\eta)\hat{\theta} - (f'')\hat{p}' \\ & + \xi^2(\hat{\theta}_t - \hat{p}_z\hat{\theta}_z) + \tfrac{1}{2}(\xi\hat{\theta}_\xi - \eta\hat{\theta}')\hat{\theta} - \hat{p}'\hat{\theta}' + \xi\hat{\theta}\hat{\theta}',\end{aligned} \tag{3.2 b}$$

where all the nonlinear terms have been retained.

At this point, we see that the disturbance equations given in (3.2) form a nonlinear set of parabolic equations, which have been derived using the limit $\delta \to 0$ as the only approximation. Therefore, equations (3.2) form a fully non-parallel and mathematically rigorous set of equations. It is well known (Nield & Bejan 1999; Rees 1998) that the primary mode of instability for the boundary-layer flow from a uniform temperature inclined surface takes the form of streamwise vortices. The remainder of this paper discusses the linear development of such vortices and therefore, given the form of (3.2), they may be Fourier-decomposed into discrete spanwise components. Upon linearization and introduction of the ansatz

$$\hat{p}(\xi, \eta, z, t) = p(\xi, \eta)\mathrm{e}^{\mathrm{i}kz}, \qquad \hat{\theta}(\xi, \eta, z, t) = \theta(\xi, \eta)\mathrm{e}^{\mathrm{i}kz}, \tag{3.3}$$

where we also assume that the flow is steady with time, equations (3.2) reduce to the form

$$p'' - k^2\xi^2 p = \tfrac{1}{2}(\xi\theta_\xi - \eta\theta') + \xi\theta', \tag{3.4 a}$$

$$\theta'' - k^2\xi^2\theta = (\tfrac{1}{2}f')\xi\theta_\xi - (\tfrac{1}{2}f)\theta' + (\xi - \tfrac{1}{2}\eta)f''\theta - f''p'. \tag{3.4 b}$$

A study of the fully nonlinear system (3.2) will be given in subsequent papers.

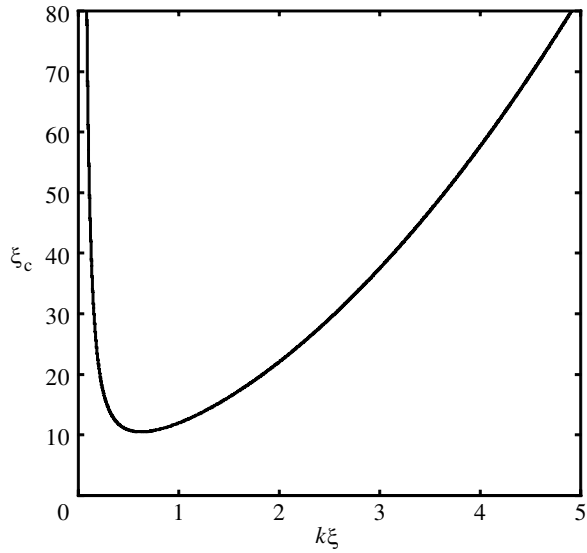

Figure 2. Neutral stability curve: ξ_c against $k\xi$.

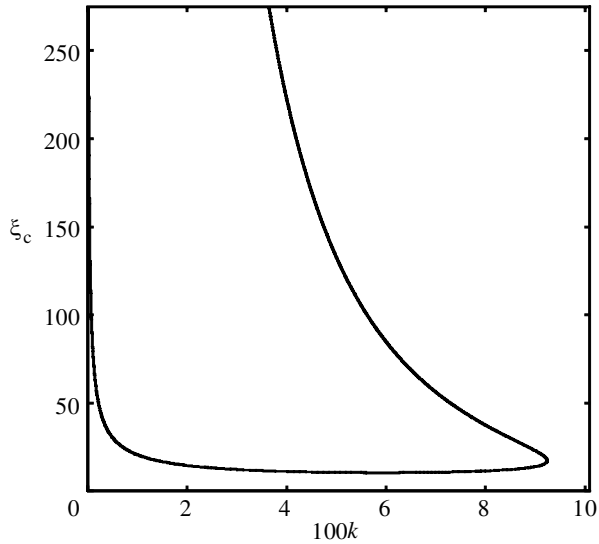

Figure 3. Neutral stability curve: ξ_c against k.

4. A straightforward linearized analysis

Equations (3.4) form a parabolic system of equations for the linear development of disturbances to the basic flow, as may be seen by the presence of ξ-derivatives. In this section we will determine the points of neutral stability that correspond to the setting of these ξ-derivatives to zero. If it were to be objected that such a procedure is arbitrary, then it has to be admitted that it is, and we will be solving the full system (3.4) later in the paper in order to compare the results. However, very many papers dealing with the stability of boundary-layer flows invoke assumptions like this.

Table 1. *Critical values for the present stability problem compared with those of Storesletten & Rees (1998) and Hsu & Cheng (1979)*

	ξ_c	x_c	k_c	$(k\xi)_c$
current	10.479 69	109.824	0.057 446	0.602 01
Storesletten & Rees (1998)	10.519 19	110.653	0.059 185	0.622 58
Hsu & Cheng (1979)	10.988 41	120.745	0.057 759	0.634 68

Therefore, we solve the following equations,

$$p'' - k^2\xi^2 p = -\tfrac{1}{2}\eta\theta' + \xi\theta', \tag{4.1 a}$$

$$\theta'' - k^2\xi^2\theta = -(\tfrac{1}{2}f)\theta' + (\xi - \tfrac{1}{2}\eta)f''\theta - f''p', \tag{4.1 b}$$

subject to the boundary conditions

$$\eta = 0: \quad p' = 0, \quad \theta = 0,$$
$$\eta \to \infty: \quad p, \theta \to 0.$$

As this homogeneous system forms an eigenvalue problem for ξ in terms of the wavenumber, k, it is necessary to supply the normalizing condition, $\theta' = 1$ at $\eta = 0$. This extra boundary condition means that we may solve (4.1 *a*) and (4.1 *b*) together with $\xi' = 0$ (where ξ is regarded as an eigenvalue). A suitably extended version of the Keller-box method was used to solve this eigensystem (see Lewis *et al.* 1997 for details). It was found necessary to perform a parameter sweep over different values of $k\xi$, rather than k, since the neutral curve in terms of k is not single valued. The results of our computations are displayed in figures 2 and 3. Figure 2 shows the variation of ξ_c with $k\xi$ and this displays the usual behaviour for a Bénard-like problem in that there is a well-defined minimum value, and that ξ_c, the critical value of ξ, becomes unbounded in the limits $k\xi \to 0$ and $k\xi \to \infty$. The detailed numerical results (not shown) also indicate that the neutral disturbance becomes confined to a narrow region close to the heated surface when $k\xi$ is large. Figure 3 displays the variation of ξ_c with k. Here we see that there is a maximum wavenumber beyond which all disturbances are stable; this value is *ca.* 0.092 36. The minimum value of ξ_c was obtained by solving (4.1) augmented by the system obtained by differentiating (4.1) with respect to k and setting $\partial\xi/\partial k = 0$; in this case, we used a fourth-order Runge–Kutta code together with a standard shooting method for two-point boundary-value problems. Table 1 shows how the present minimization compares with others in the literature.

The fact that the current value of ξ_c is smaller than those of the other quoted papers is of little consequence. Storesletten & Rees (1998) and Hsu & Cheng (1979) made different assumptions about which terms should be kept in the linearized stability equations, and given that the flows considered by those authors were from generally inclined surfaces, the computation of a critical distance negates the initial assumption that the boundary-layer approximation is valid. In the present problem, the assumption that the surface is nearly vertical implies that the disturbance equations automatically satisfy the boundary-layer approximation.

For purposes of comparison, we reproduce in the current notation the disturbance equations solved by the various authors already quoted in order to indicate the

sources of discrepancy between the above results. The present analysis solves the equations

$$p'' - k^2\xi^2 p = -\tfrac{1}{2}\eta\theta' + \xi\theta',$$
$$\theta'' - k^2\xi^2\theta = -(\tfrac{1}{2}f)\theta' + (\xi - \tfrac{1}{2}\eta)f''\theta - f''p',$$

which are equations (4.1), whereas Storesletten & Rees (1998) solve

$$p'' - k^2\xi^2 p = \xi\theta', \tag{4.2 a}$$
$$\theta'' - k^2\xi^2\theta = \tfrac{1}{2}(\eta f' - f)\theta' + (\xi - \tfrac{1}{2}\eta)f''\theta - f''p'. \tag{4.2 b}$$

The two terms which form the difference between these two sets of equations find their origin in the different treatments of the x-variation of the disturbance. The analysis leading to (4.2) assumes no x-variation before the variables are transformed from Cartesian coordinates to the similarity variables, while the present analysis makes no such assumption until the full disturbance equations are found.

Hsu & Cheng (1979) assume that the vortex disturbances are independent of the streamwise coordinate and therefore it is possible to define a streamfunction in the yz-plane, which we will denote by Ψ. Their equations are

$$\Psi'' - k^2\xi^2\Psi = -k\xi\theta, \tag{4.3 a}$$
$$\theta'' - k^2\xi^2\theta = -\tfrac{1}{2}f\theta' - \tfrac{1}{2}\eta f''\theta + k\xi f''\Psi, \tag{4.3 b}$$

while those of the present analysis are

$$\Psi'' - k^2\xi^2\Psi = -k\xi\theta, \tag{4.4 a}$$
$$\theta'' - k^2\xi^2\theta = \tfrac{1}{2}(\eta f' - f)\theta' - \tfrac{1}{2}\eta f''\theta + k\xi f''\Psi. \tag{4.4 b}$$

These systems differ from each other for the same reason as above. Equations (4.1) and (4.4) were checked carefully and they yield precisely the same numerical solution. However, equations (4.2) and (4.3) yield different solutions, not only from those of (4.1) and (4.4), but also from one another. Although both were derived using the assumption of no x-variation, equation (4.2) assumes that p is independent of x, whereas ψ is independent of x in (4.3); these are essentially different assumptions, and this reflects the inconsistency of the approach.

5. Parabolic linearized analysis

The main assumption used in the last section, namely that all ξ-derivatives may be set to zero, is not necessarily valid, and therefore we need to perform a full parabolic simulation of the linearized disturbance equations (3.4). This is readily undertaken using the Keller-box method introduced by Keller & Cebeci (1971). Further details of the implementation, which is more advanced than the standard implementation described in Cebeci & Bradshaw (1984), is as follows. We use a backward difference discretization in ξ, rather than a central difference approximation, in order to maximize numerical stability. The Jacobian matrix used in the central Newton–Raphson procedure is computed numerically within the code, rather than specified explicitly by the programmer; this increases substantially the speed of implementation of the method. In our results we have used uniform grids in both the ξ- and η-directions

with 400 intervals specified in the range $0 \leqslant \xi \leqslant 40$ and 50 intervals in $0 \leqslant \eta \leqslant 10$. In our simulation we solved (4.1) subject to the boundary conditions

$$\left.\begin{aligned} \eta = 0: \quad & p' = 0, \quad \theta = 0, \\ \eta \to \infty: \quad & p, \theta \to 0. \end{aligned}\right\} \tag{5.1}$$

A thermal disturbance of the form

$$\theta = \eta \mathrm{e}^{-\eta} \tag{5.2}$$

was introduced at various values of ξ and the Keller-box method was used to march this disturbance forward in space. It was not necessary to determine a corresponding initial profile for p because (i) the method is a backward difference method and (ii) there are no ξ-derivatives of p in the equations; these two facts mean that the numerical solution at the next streamwise location in the boundary layer does not use the p distribution at the previous location.

In the context of the classical Darcy–Bénard convection problem, instability occurs when disturbances grow in time. In the present problem, we may define instability to occur when disturbances grow in space. However, the Darcy–Bénard problem has no ambiguity in how instability is defined; the use of the maximum disturbance temperature, surface rate of heat flux or disturbance energy as measures of growth are entirely equivalent. In boundary-layer flows, these different measures of instability give different results, and therefore we have monitored the magnitude of all three. The maximum temperature at each value of ξ was obtained by locating the maximum value over all the gridpoints, fitting a parabolic curve to that point and its two nearest neighbours, and finding the maximum value on that curve. The surface rate of heat transfer is measured in terms of $\theta_y = \xi\theta_\eta$ at $\eta = 0$ (noting that values of θ_η at $\eta = 0$ yield less restrictive curves than does θ_y at $y = 0$ in all cases). Finally, the thermal energy of the disturbance is deemed to be proportional to

$$E = \int_0^\infty \theta \, \mathrm{d}y = \xi \int_0^\infty \theta \, \mathrm{d}\eta. \tag{5.3}$$

In this last case, neutral stability may be said to occur when E attains maximum or minimum values as ξ increases. These correspond to where

$$\frac{\mathrm{d}E}{\mathrm{d}x} = \frac{1}{2\xi}\frac{\mathrm{d}E}{\mathrm{d}\xi} = 0. \tag{5.4}$$

Therefore, we determine by linear interpolation those points at which

$$\frac{\mathrm{d}E}{\mathrm{d}\xi} = \int_0^\infty \left(\xi \frac{\partial\theta}{\partial\xi} + \theta\right) \mathrm{d}\eta = 0. \tag{5.5}$$

The typical evolutions of the disturbance energies, E, are shown in parts (a) and (b) of figure 4; these correspond, respectively, to values of k which are less than, equal to or greater than 0.07. Also depicted are the extreme values of these curves, to indicate clearly how the value of ξ corresponding to neutrality varies with the wavenumber. In these figures, the disturbance was introduced at $\xi = 1$ and the energy of the disturbance decreases at first before increasing again. In figure 4a we see that, for values of k less than 0.05, the critical value of ξ decreases at first with increasing

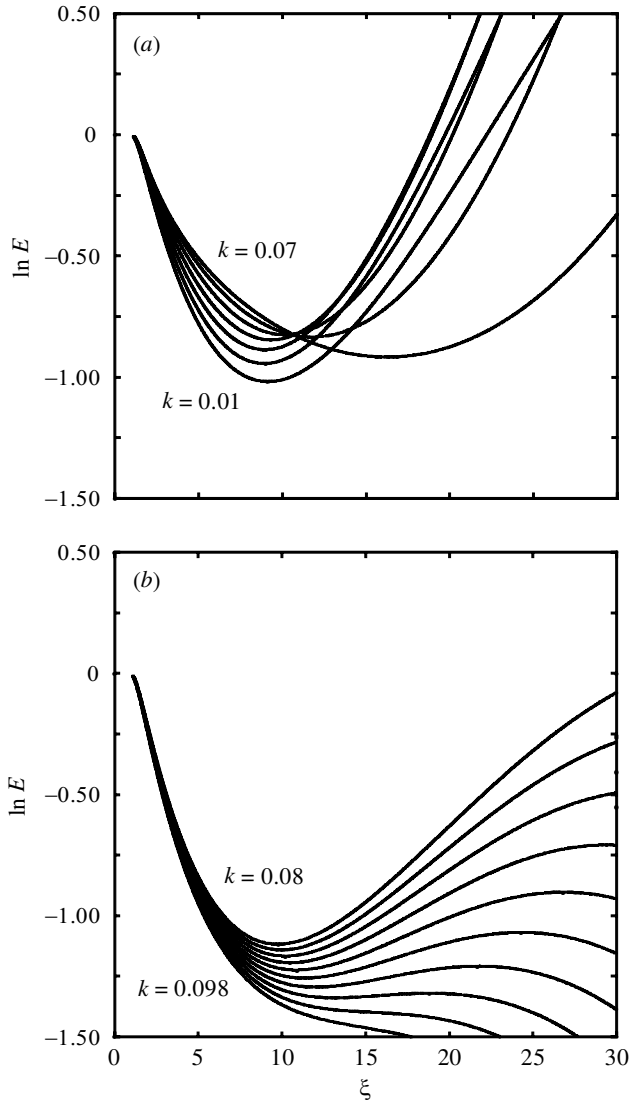

Figure 4. (*a*) Variation of $\ln E$ against ξ for $k = 0.01, 0.02, \ldots, 0.07$. The symbol • denotes maximum values of E. (*b*) Variation of $\ln E$ against ξ for $k = 0.08, 0.083, \ldots, 0.098$. The symbol • denotes maximum values of E.

k and then it increases for larger values of k. In figure 4*b* we see a second neutral location for a certain range of wavenumbers; these correspond to points marking the re-establishment of stability. When $k > 0.094$, the energy always decays and therefore the flow is stable. Similarly shaped curves are obtained for the evolution of the maximum temperature and the surface rate of heat transfer. Likewise, similar curves are also computed for other initial disturbance profiles.

The curves shown in figure 4, and those corresponding to the other two monitoring functions, are summarized in figures 5–7. Figure 5 corresponds directly to figure 4, as the disturbance is introduced at $\xi = 1$. But figures 6 and 7 correspond to disturbances

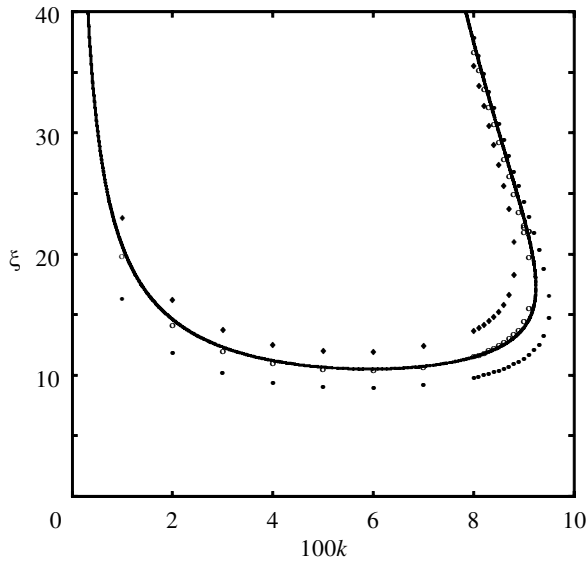

Figure 5. Neutral stability giving ξ_c as a function of k where the disturbance is introduced at $\xi = 1$. The continuous curve is the same as that displayed in figure 3. The symbol • represents the thermal energy stability criterion. The symbol ∘ represents the maximum temperature criterion. The symbol ♦ represents the surface heat flux criterion.

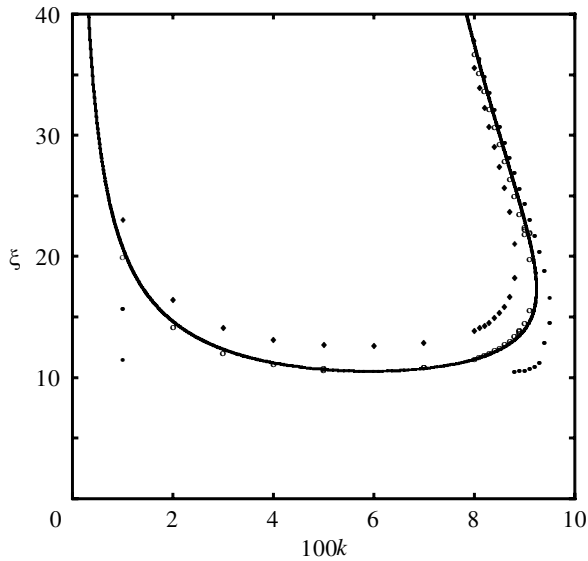

Figure 6. As figure 5, but with disturbance having been introduced at $\xi = 10$.

introduced at $\xi = 10$ and 20, respectively. A further computation was undertaken for $\xi = 5$, but the results were virtually indistinguishable from the $\xi = 1$ results. In all three figures, the neutral stability curve shown in figure 3 has been reproduced for reference. Referring to figure 5, we see that the criterion based on the thermal energy of the disturbance yields a curve with a lower minimum than those based on the other two criteria, and that instability also occurs for a larger range of wavenumbers. Some

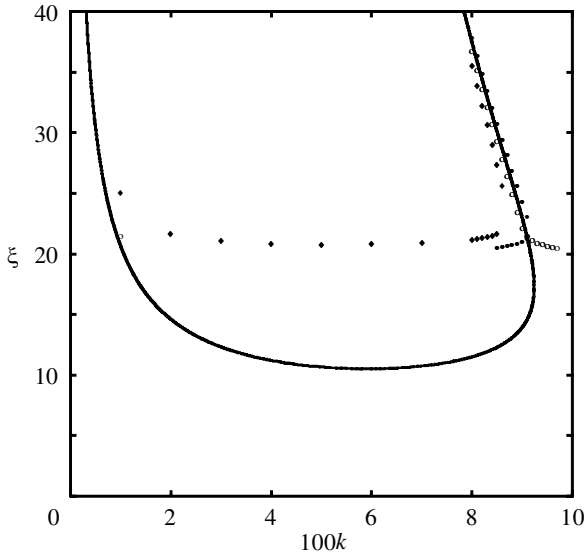

Figure 7. As figure 5, but with disturbance having been introduced at $\xi = 20$.

further computations were undertaken to find more precisely at which wavenumber the earliest onset criterion may be found. This was determined to be at $\xi \simeq 8.970$ (i.e. $x \simeq 80.46$) at a wavenumber of approximately $k = 0.057\,23$; these values should be compared with those given in table 1. Both the maximum temperature and energy-based criteria yield a minimum critical Rayleigh number below that of the simplified linearized analysis discussed in § 4, in which the ξ-derivatives were neglected. Clearly, the onset of convection does not correspond to $\theta_\xi = 0$ everywhere, but is firmly dependent on how the disturbance evolves.

When the disturbance is introduced at $\xi = 10$, the disturbance grows immediately for $k < 0.88$ according to the energy-based criterion, which explains the disappearance of the data points in figure 6. This effect is stronger in figure 7, where $\xi = 20$ is the point of introduction of the disturbance. Here the maximum temperature criterion grows initially in all cases except for $k = 0.01$. In view of the critical values of ξ displayed in figure 5, it is not surprising that this should happen, as the disturbance is introduced into the boundary layer well beyond where it may become unstable.

In all three cases, and for all three criteria, the neutral curves seem to become increasingly close to the simplified neutral curve as the right-hand branch is traversed upwards, although the curve corresponding to the energy-based criterion is the closest of the three methods in this regard.

6. Discussion

In this paper we have put forward what are the first steps in discussing a consistent vortex stability analysis for free convective boundary-layer flows from inclined surfaces in porous media. Mathematical consistency is ensured in this case by requiring the heated surface to be asymptotically close to being vertical, and this means that the boundary-layer approximation is valid for both the basic flow and the linearized disturbance equations. Indeed, this is also true for the fully nonlinear disturbance equations, although we have not considered that aspect here.

We find that a straightforward analysis based on an *a priori* specification of the streamwise variation of the disturbance restricts the flow to such an extent that it overestimates the point of neutral stability compared with that obtained using parabolic simulations. The qualitative behaviour of the stability characteristics, however, are preserved.

Although we have presented a mathematically consistent analysis, the configuration studied is specialized and it is of interest to determine what happens at other inclination angles. In general, it is not possible to follow the same analytical procedure and therefore numerical methods must be used to solve the full equations. Unsteady nonlinear wave instabilities for the horizontal boundary layer have been computed by Rees & Bassom (1993), and these authors have found that convection becomes chaotic immediately. For the vertical case, the numerical simulation of Rees (1993) and the asymptotic analysis of Lewis *et al.* (1995) suggest very strongly that wave instabilities are absent. In the more general case of a porous medium without local thermal equilibrium between the fluid and solid phases, numerical simulations of the vertical boundary layer also suggest stability (see Rees 1999). Work is in progress on developing an unsteady three-dimensional code to simulate nonlinear vortex development for generally inclined boundary layers.

Finally, we emphasize again the fact that the analysis above shows that fully nonlinear vortex development may also be described within this parabolic framework, the only approximation being the boundary-layer approximation. Detailed numerical analyses of the nonlinear spatial evolution of vortices and their secondary instabilities are in progress and will be presented in companion papers.

The author thanks the anonymous referees for their very useful comments.

References

Cebeci, T. & Bradshaw, P. 1984 *Physical and computational aspects of convective heat transfer*. Springer.

Cheng, P. & Minkowycz, W. J. 1977 Free convection about a vertical flat plate imbedded in a porous medium with application to heat transfer from a dike. *J. Geophys. Res.* **82**, 2040–2044.

Hall, P. 1983 The linear development of Görtler vortices in growing boundary layers. *J. Fluid Mech.* **130**, 41–58.

Hsu, C. T. & Cheng, P. 1979 Vortex instability in buoyancy induced flow over inclined heated surfaces in porous media. *Trans. ASME J. Heat Transfer* **101**, 660–665.

Jang, J. Y. & Chang, W. J. 1988 Vortex instability of buoyancy-induced inclined boundary-layer flow in a saturated porous-medium. *Int. J. Heat Mass Transfer* **31**, 759–767.

Keller, H. B. & Cebeci, T. 1971 Accurate numerical methods for boundary layer flows 1. Two-dimensional flows. In *Proc. 2nd Int. Conf. Numerical Methods in Fluid Dynamics*, Lecture Notes in Physics, pp. 92–100. Springer.

Lewis, S., Bassom, A. P. & Rees, D. A. S. 1995 The stability of vertical thermal boundary layer flow in a porous medium. *Eur. J. Mech.* B **14**, 395–408.

Lewis, S., Rees, D. A. S. & Bassom, A. P. 1997 High wavenumber convection in tall porous containers heated from below. *Q. J. Mech. Appl. Math.* **50**, 545–563.

Nield, D. A. & Bejan, A. 1999 *Convection in porous media*, 2nd edn. Springer.

Rees, D. A. S. 1993 Nonlinear wave stability of vertical thermal boundary layer flow in a porous medium. *J. Appl. Math. Phys.* **44**, 306–313.

Rees, D. A. S. 1998 Thermal boundary layer instabilities in porous media: a critical review. In *Transport phenomena in porous media* (ed. D. B. Ingham & I. Pop). Oxford: Pergamon.

Rees, D. A. S. 1999 Vertical free convection boundary-layer flow in a porous medium using a thermal nonequilibrium model: elliptic effects. In *Proc. of the Workshop on Applied Mathematics, Sylhet, Bangladesh, 1–3 September 1998*, pp. 13–22.

Rees, D. A. S. & Bassom, A. P. 1993 The nonlinear nonparallel wave instability of boundary-layer flow-induced by a horizontal heated surface in porous media. *J. Fluid Mech.* **253**, 267–295.

Riley, D. S. & Rees, D. A. S. 1985 Non-Darcy natural convection from arbitrarily inclined heated surfaces in saturated porous media. *Q. J. Mech. Appl. Math.* **38**, 277–295.

Storesletten, L. & Rees, D. A. S. 1998 The influence of higher–order effects on the linear instability of thermal boundary layer flow in porous media. *Int. J. Heat Mass Transfer* **41**, 1833–1843.